Moment-SOS Approach to Interval Power Flow

Chao Duan, *Student Member, IEEE*, Lin Jiang, *Member, IEEE*, Wanliang Fang, Jun Liu, *Member, IEEE*

***Abstract*—Intermittent renewable sources and market-driven operation have brought many uncertainties into modern power systems. Power flow analysis tools are expected to be able to incorporate uncertainties into the solution process. Interval power flow (IPF) analysis which aims at obtaining the upper and lower bounds of power flow solutions under interval uncertainties, thereby emerges as a promising framework to meet such expectation. This paper describes a novel optimization-based method to obtain high-accuracy or even exact global solutions to IPF problems. At first, the IPF problems are formulated as polynomial optimization problems probably with rational objective functions. Then Lasserre's hierarchy, or moment-SOS approach, is introduced to relax the non-convex problems to convex semidefinite programming (SDP) problems. Correlative sparsity in the polynomial optimization problems is exploited to improve numerical tractability and efficiency. Finally, case studies on IEEE 6-bus, 9-bus and 14-bus systems demonstrate the second-order moment relaxation is capable of obtaining exact global interval solutions on small-scale systems, and numerical results on IEEE 57-bus, 118-bus and 300-bus systems show the proposed method can significantly improve the interval solutions compared with recent Linear Programming (LP) relaxation method on larger systems.**

***Index Terms*—Interval power flow, polynomial optimization, moment relaxation, correlative sparsity.**

I. Introduction

Integration of intermittent renewable sources and advent of deregulated competitive power markets increase the uncertainties of power system operation. It will be more and more difficult to acquire reliable information of steady-state operation by just running the conventional power flow (PF) program. There is a long-recognized and pressing need for power flow analysis tools to consider uncertainties.

Power flow analysis methods in the presence of uncertainty can be classified into two groups according to how uncertainty is represented. The first group is the probabilistic power flow (PPF) in which loads and generations are expressed as random variables with associated distribution functions. PPF aims at deriving the probability distribution of power flow solutions. Monte Carlo simulation based techniques [1], [2], analytical methods [3]–[5] and point estimate methods [6], [7] are extensively investigated to deal with this problem. However, this group of methods depends on the assumption that the random behavior of uncertainty obeys pre-defined distribution which is difficult to identify in practice.

The second group of methods, interval power flow (IPF) [8]–[12], model uncertainty of loads and generations as intervals without distribution structures, which seems a more practical approach because system operators need to consider the worst-case scenario to guarantee the security of the power networks. Interval arithmetic (IA) is introduced in [8] to modify conventional Newton iterations to obtain outer approximation of the solution set, but the results are highly conservative and the convergence is unfounded. A local search procedure is proposed in [9] to find accurate boundary solutions but the convergence is not proved and only local optimality is guaranteed. To overcome the limitation of the IA method, affine arithmetic (AA) is used in [10] by expressing power system state variables as affine function of uncertainties, and linear programming (LP) is employed to obtain tight bounds of uncertainty parameters. However, this method is still approximate in nature. In [11], from a range arithmetic perspective, a nonlinear programming (NLP) model with complementarity constraints is proposed to find the upper and lower bounds of power flow solutions. Although the formulation is non-convex and difficult to solve, this work provides a theory foundation for optimization-based method to solve IPF. In the most recent work [12], IPF is formulated as a quadratically constrained quadratic programming (QCQP) problem. Convex envelops are employed to relax the non-convex QCQP to a convex LP. Starting from estimated solution intervals, the optimality-based bounds tightening (OBBT) method is introduced to obtain the tight outer approximation of the feasible region. Though this method can obtain less conservative interval solutions than previous methods, the results in any case are still supersets of the exact intervals.

The method used in [12] belongs to a class of methods named convex relaxation. The general idea is to enlarge the feasible sets by lifting the non-convex problems into a higher dimensional space where they are convex [13]. Then the convex problems are solved and the solutions are projected back onto the original space. These methods generally provide lower (upper) bounds for min. (max.) problems. When the projected solutions happen to lie in the feasible sets of the original problems, they obtain the global solutions of the original problems. This idea attracts much attention in optimal power flow (OPF) problems. After the seminal paper [14] making the important observation that SDP relaxation can find the global optimal solutions for several benchmark systems, much work has been devoted to the exactness conditions [15], [16] and implementation issues [17], [18] of convex, especially SDP relaxation of OPF. As conventional SDP relaxation is not always exact for the OPF problems, people are still seeking for tighter convex relaxations. Recent development

This work was supported in part by Engineering and Physical Sciences Research Council (EP/L014351/1) and in part by the National Natural Science Foundation of China (No. 51428702). *(Corresponding author: Wanliang Fang.)*

C. Duan, W. Fang and J. Liu are with the Department of Electrical Engineering, Xi'an Jiaotong University, Xi'an 710049, China. C. Duan is also with Department of Electrical Engineering and Electronics, University of Liverpool, Liverpool L69 3GJ, U.K. (e-mail: duanchao@stu.xjtu.edu.cn; eewlfang@mail.xjtu.edu.cn ; eeliujun@mail.xjtu.edu.cn)

L. Jiang is with Department of Electrical Engineering and Electronics, University of Liverpool, Liverpool L69 3GJ, U.K. (e-mail: ljiang@liverpool.ac.uk)

in polynomial optimization provides a moment-SOS (sum of squares) approach to construct a hierarchy of SDP relaxations whose optima asymptotically [19] and often finitely [20] converge to the global optimum of the original non-convex problem. This approach has already been applied to OPF problems and obtained the global solutions of some cases where the conventional SDP method failed [21]–[23]. Due to the similarity in problem formulation, moment-SOS approach has the potential to tackle IPF problem as well.

The contribution of this paper is applying sparsity-exploiting moment-SOS approach to IPF problems. Previous methods for IPF, in any case, can only obtain either outer approximation (e.g. IA, AA and LP relaxation methods) or inner approximation (e.g. Monte Carlo method) of the true intervals. In contrast, the moment-SOS approach can obtain the theoretically guaranteed exact interval solutions on small-scale systems. For larger systems, moment-SOS approach can also be employed to further tighten the interval solutions obtained by other methods, e.g. LP relaxation method [12], when high accuracy bounds are needed.

The rest of this paper is organized as follows. Mathematical notations and definitions used in the manuscript are described in section II. The polynomial optimization formulation of IPF problems is presented in section III. Section IV introduces the moment relaxation of IPF problems and section V describes the sparse techniques in moment relaxation. Case studies are reported in section VI. Finally, section VII draws conclusions and gives suggestions on future research.

II. Notation and Definition

Let $\mathbb{R}$ be the set of real numbers, and $\mathbb{N}$ the set of nonnegative integers. $\mathbb{R}^n$ and $\mathbb{N}^n$ denote the sets of n-dimensional real and integer vectors, respectively. Boldface lower case letter $\boldsymbol{a}$ denotes a real vector with lowercase letter a_i denoting its i^{th} scalar element. $\mathbb{N}^n_d = \{\boldsymbol{\alpha} \in \mathbb{N}^n | \sum_{i=1}^n \alpha_i \leq d\}$ for $d \in \mathbb{N}$. Parentheses are used to construct vectors from comma separated lists as $(\boldsymbol{x}_1, \ldots, \boldsymbol{x}_k) = (\boldsymbol{x}_j)_{1\leq j\leq k} = [\boldsymbol{x}_1^T, \ldots, \boldsymbol{x}_k^T]^T$. Calligraphic uppercase letter $\mathcal{A}$ denotes a index set and $|\mathcal{A}|$ is its cardinality, i.e. number of elements. Matrix $A \succcurlyeq \mathbf{0}$ means that A is positive semidefinite. $\lceil x \rceil$ denotes the smallest integer greater than or equal to x.

$\mathbb{R}[\boldsymbol{x}]$ denotes the set of real valued polynomials in $x_i, i = 1, \ldots, n$. Each polynomial $f \in \mathbb{R}[\boldsymbol{x}]$ is represented as $f(\boldsymbol{x}) = \sum_{\boldsymbol{\alpha}\in\mathcal{F}} c(\boldsymbol{\alpha})\boldsymbol{x}^{\boldsymbol{\alpha}}$ for a finite set $\mathcal{F} \in \mathbb{N}^n$ and some real numbers $c(\boldsymbol{\alpha})$ where $\boldsymbol{x}^{\boldsymbol{\alpha}} = x_1^{\alpha_1} x_2^{\alpha_2} \ldots x_n^{\alpha_n}$ and $\mathcal{F}$ denotes the set of index vector related to its monomials. The set $\mathcal{F}$ is also called the set of supports denoted as $\text{supp}(f)$. The degree of $f \in \mathbb{R}[\boldsymbol{x}]$ is denoted by $\deg(f) = \max\{\sum_{i=1}^n \alpha_i | \boldsymbol{\alpha} \in \text{supp}(f)\}$.

A clique of a undirected graph $G(\mathcal{N}, \mathcal{E})$ is a subset of vertices such that its induced subgraph is complete, i.e. there is a edge between every two distinct vertices. A maximal clique is a clique that is not a proper subset of another clique. A chord is any edge joining two nonconsecutive vertices of a cycle. An undirected graph is chordal if every cycle of length greater than three has a chord. A graph $G(\mathcal{N}, \overline{\mathcal{E}})$ is a chordal extension of $G(\mathcal{N}, \mathcal{E})$ if it is a chordal graph and $\mathcal{E} \subseteq \overline{\mathcal{E}}$.

III. IPF Problem Formulation

In this section, IPF problems are formulated as polynomial optimization problems. Consider a power network with n_b buses and n_l lines. $\mathcal{N}$ denotes the set of bus indexes and $\mathcal{L}$ is the set of line indexes. $\mathcal{N}_{pv}$ and $\mathcal{N}_{pq}$ denote the index sets for PV and PQ buses, respectively. To obtain a polynomial formulation, bus voltages are expressed in rectangular coordinates. Let e_k and f_k denote the real and imaginary parts of complex bus voltage of bus k. Further define $\boldsymbol{v}_k = (e_k, f_k)$ and $\boldsymbol{v} = (\boldsymbol{v}_k)_{k\in\mathcal{N}}$. Without loss of generality, the first bus is assumed to be the reference bus and set $f_1 = 0$. The $(j,k)^{th}$ element of the network admittance matrix is denoted by $g_{jk} + \mathrm{j}b_{jk}$. Due to the uncertainty of loads and generations, the exact values of power injections are unknown whereas the estimated intervals are available. When the power injections stay in the estimated intervals, the power flow solutions must also be within certain intervals. IPF hence aims to obtain the the upper and lower bounds for power flow solutions, formally stated as the following optimization problem:

$$\min_{\boldsymbol{v}}(\max)\ f(\boldsymbol{v}) \qquad \text{subject to} \tag{1a}$$

$$\underline{P}_k \leq e_k \sum_{j=1}^{n_b}(g_{jk}f_j - b_{jk}e_j) + f_k \sum_{j=1}^{n_b}(g_{jk}e_j + b_{jk}f_j) \leq \overline{P}_k, \quad \forall k \in \mathcal{N}_{pv} \cup \mathcal{N}_{pq} \tag{1b}$$

$$\underline{Q}_k \leq f_k \sum_{j=1}^{n_b}(g_{jk}f_j - b_{jk}e_j) - e_k \sum_{j=1}^{n_b}(g_{jk}e_j + b_{jk}f_j) \leq \overline{Q}_k, \quad \forall k \in \mathcal{N}_{pq} \tag{1c}$$

$$e_k^2 + f_k^2 = U_k^2, \qquad \forall k \in \mathcal{N}_{pv} \tag{1d}$$

$$e_1 = U_1,\ f_1 = 0 \tag{1e}$$

$$e_k^2 + f_k^2 \geq V_m^2, \qquad \forall k \in \mathcal{N} \tag{1f}$$

where the objective $f(\boldsymbol{v})$ can be voltage magnitude (V.M.) $e_k^2 + f_k^2$, voltage angle (V.A.) f_k/e_k, line active power (A.P.)

$$g_{ij}(e_i^2 + f_i^2) - (e_i g_{ij} e_j - e_i b_{ij} f_j + f_i g_{ij} f_j + f_i b_{ij} e_j) \tag{2}$$

and line reactive power (R.P.)

$$-b_{ij}(e_i^2 + f_i^2) - (f_i g_{ij} e_j - f_i b_{ij} f_j - e_i g_{ij} f_j - e_i b_{ij} e_j). \tag{3}$$

Note that the rational function f_k/e_k is used for voltage angle because there is a bijection between f_k/e_k and $\text{atan}(f_k/e_k)$ and the moment-SOS approach discussed later allows for an elegant way to deal with rational objectives. It is well known that there exist some low voltage solutions to the power flows equations which are strongly related to voltage instability [24]. The inequality constraint (1f) is thereby added to exclude such unrealistic operational points. Problem (1) is a non-convex optimization problem for which conventional interior point method can only guarantee a local minimum. Similar to what happened to OPF problems, global solutions can be obtained by proper convex relaxations.

Problem (1) is a direct extension of conventional power flow (PF) problem. Loads and generations are modelled as nodal power injections. Buses are classified into three types, e.g. PQ, PV and slack buses [25]. Active and Reactive power injection limits are set for PQ buses. PV buses entail active

power injection limits and fixed voltage magnitudes. Slack bus is taken as voltage reference point with fixed complex voltage. Similar to PF, after solving IPF (1), if the reactive power injections at some PV buses exceed their available reactive power upper (lower) limits, those PV buses will be converted to PQ buses by just setting the reactive power injections as the upper (lower) limits. Then the problem is solved again. This process is repeated until no reactive power injection limits at PV buses are violated. Flowchart of this procedure is given in [12].

IV. Moment Relaxations of IPF Problems

Moment-SOS approach can be understood from two viewpoints. The first viewpoint is based on the sum-of-squares (SOS) representation of nonnegative polynomials [26]. The second one considers polynomial optimization problems as generalized moment problems [19] [27]. These two viewpoints are actually a primal and dual pair in the sense of a generalize lagrangian function [28] and their generated SDPs also maintain a primal-dual relationship. In practice, the moment viewpoint is often adopted because it offers easily checkable conditions to certify the exactness of the SDP relaxations.

Consider a compact form of problem (1): minimizing a polynomial objective function $f(\boldsymbol{v})$ (1a) over a compact set $\mathbb{K} \subset \mathbb{R}^n$ defined by a tuple of polynomial equalities $\{h_m(\boldsymbol{v}) = 0\}_{m\in\mathcal{E}}$ (1d,1e) and inequalities $\{g_n(\boldsymbol{v}) \geq 0\}_{n\in\mathcal{I}}$ (1b,1c,1f). We first explain the method for polynomial objective functions and the modification needed for rational objective functions will be mentioned later. The moment approach is based on the observation that problem

$$\min_{\boldsymbol{v}\in\mathbb{K}} f(\boldsymbol{v}) \tag{4}$$

is equivalent to

$$\min_{\mu\in\mathscr{M}(\mathbb{K})_+} \int_{\mathbb{K}} f d\mu \text{ s.t.} \int_{\mathbb{K}} d\mu = 1 \tag{5}$$

where $\mathscr{M}(\mathbb{K})_+$ is the set of all non-negative measures on $\mathbb{K}$. Let f^* and ρ^* be the minimums of the problem (4) and (5), respectively. The equivalence of the above two problems is trivial: $f(x) \geq f^*$ on $\mathbb{K}$ implies $\int_{\mathbb{K}} f d\mu \geq f^*$, therefore $f^* \leq \rho^*$; take $\mu = \delta_{x^*}$ which is the Dirac measure at the minimizer of the first problem, then $\rho^* \leq \int_{\mathbb{K}} f d\delta_{x^*} = f^*$. Note that problem (4) is generically nonlinear and nonconvex while problem (5) is always convex though infinite dimensional. Therefore problem (5) is the main focus in the sequel.

The restrictive structure of polynomials enable us characterize the measure on $\mathbb{K}$ with a infinite sequence of moments, i.e. $\boldsymbol{y} = (y(\boldsymbol{\alpha}))_{\boldsymbol{\alpha}\in\mathbb{N}^{2n_b}}$ with $y(\boldsymbol{\alpha}) = \int_{\mathbb{K}} \boldsymbol{v}^{\boldsymbol{\alpha}} d\mu$ for some $\mu \in \mathscr{M}(\mathbb{K})_+$. Therefore, the unknown measure in problem (5) can be replaced by its sequence of moments $\boldsymbol{y}$. Define the Riesz linear functional $L_{\boldsymbol{y}} : \mathbb{R}[\boldsymbol{v}] \mapsto \mathbb{R}$ associated with a moment sequence $\boldsymbol{y}$ as $f(\boldsymbol{v}) = \sum_{\boldsymbol{\alpha}\in\mathbb{N}^n} c(\boldsymbol{\alpha})\boldsymbol{v}^{\boldsymbol{\alpha}} \mapsto L_{\boldsymbol{y}}(f) = \sum_{\boldsymbol{\alpha}\in\mathbb{N}^n} c(\boldsymbol{\alpha}) y^{\boldsymbol{\alpha}}$. Thus, problem (5) is transformed to

$$\min_{\boldsymbol{y}\in\mathbb{R}^\infty} L_{\boldsymbol{y}}(f) \text{ s.t. } \begin{array}{l} \exists \mu \in \mathscr{M}(\mathbb{K})_+, y(\boldsymbol{\alpha}) = \int_{\mathbb{K}} \boldsymbol{v}^{\boldsymbol{\alpha}} d\mu, \forall \boldsymbol{\alpha} \in \mathbb{N}^n \\ y(\boldsymbol{0}) = 1 \end{array} \tag{6}$$

The condition under which a given sequence $\boldsymbol{y}$ is the moment sequence of some positive measure on $\mathbb{K}$ has long been studied known as the $\mathbb{K}$-moment problem [27]. To state this condition, the definitions of moment matrix and localizing matrix are needed. The moment matrix $M_d(\boldsymbol{y})$ associated with $\boldsymbol{y}$ is the real symmetric matrix with rows and columns indexed in certain monomial basis $(\boldsymbol{v}^{\boldsymbol{\alpha}})$ with entries $M_d(\boldsymbol{y})(\boldsymbol{\alpha},\boldsymbol{\beta}) = L_{\boldsymbol{y}}(\boldsymbol{v}^{\boldsymbol{\alpha}+\boldsymbol{\beta}}) = y(\boldsymbol{\alpha}+\boldsymbol{\beta})$, $\boldsymbol{\alpha},\boldsymbol{\beta} \in \mathbb{N}^n_d$. Similarly, the localizing matrix $M_d(g\boldsymbol{y})$ associated with $\boldsymbol{y}$ and polynomial $g \in \mathbb{R}[\boldsymbol{v}]$ is the real symmetric matrix with rows and columns indexed in monomial basis $(\boldsymbol{v}^{\boldsymbol{\alpha}})$ with entries $M_d(g\boldsymbol{y})(\boldsymbol{\alpha},\boldsymbol{\beta}) = L_{\boldsymbol{y}}(g(\boldsymbol{v})\boldsymbol{v}^{\boldsymbol{\alpha}+\boldsymbol{\beta}}) = \sum_{\boldsymbol{\gamma}} g_{\boldsymbol{\gamma}} y(\boldsymbol{\alpha}+\boldsymbol{\beta}+\boldsymbol{\gamma})$, $\boldsymbol{\alpha},\boldsymbol{\beta} \in \mathbb{N}^n_d$. It turns out that, under mild assumption, sequence $\boldsymbol{y}$ is a moment sequence for some positive measure on $\mathbb{K}$ if and only if $\forall d \in \mathbb{N}$, $M_d(\boldsymbol{y}) \succcurlyeq \boldsymbol{0}$, $M_d(h_m\boldsymbol{y}) = \boldsymbol{0}, \forall m \in \mathcal{E}$, $M_d(g_n\boldsymbol{y}) \succcurlyeq \boldsymbol{0}$, $\forall n \in \mathcal{I}$ [27]. To make it numerically trackable, it is necessary to relax it to a finite dimensional problem by limiting the order of monomials involved. Let $d_f = \lceil deg(f)/2 \rceil$, $d_{h_m} = \lceil deg(h_m)/2 \rceil$, $\forall m \in \mathcal{E}$ and $d_{g_n} = \lceil deg(g_n)/2 \rceil$, $\forall n \in \mathcal{I}$. For a fixed $d \geq \max\{d_f, \{d_{h_m}\}_{m\in\mathcal{E}}, \{d_{g_n}\}_{n\in\mathcal{I}}\}$, it results in the following SDP:

$$\begin{aligned}
&\min_{\boldsymbol{y}\in\mathbb{R}^{\binom{2n_b+2d}{2d}}} L_{\boldsymbol{y}}(f) && \text{subject to} && && \text{(7a)}\\
&M_d(\boldsymbol{y}) \succcurlyeq \boldsymbol{0} && && && \text{(7b)}\\
&M_{d-d_{h_m}}(h_m\boldsymbol{y}) = \boldsymbol{0} && && \forall m \in \mathcal{E} && \text{(7c)}\\
&M_{d-d_{g_n}}(g_n\boldsymbol{y}) \succcurlyeq \boldsymbol{0} && && \forall n \in \mathcal{I} && \text{(7d)}\\
&y(\boldsymbol{0}) = 1 && && && \text{(7e)}
\end{aligned}$$

Problem (7) serves as a finite dimensional relaxation and its optimum is a lower bound of that of problem (5). By increasing the relaxation order d, it leads to a hierarchy of semidefinite programs whose optima asymptotically converge to that of problem (5) [19]. Moreover, finite convergence happens in generic problems [20].

In this paper, the original polynomial optimization problem is assumed to have unique global optimum. This assumption is reasonable in practical IPF problems because the feasible sets of IPF problems are compact, thus any small random perturbation of the objective function makes its solution unique. The condition under which the order-d moment relaxation (7) is exact can then be stated as rank $M_d(\boldsymbol{y}^*) = 1$ where $\boldsymbol{y}^*$ is the optimal solution of order-d SDP realxation (7). If this condition is satisfied, the spectral decomposition of the diagonal block of $M_d(\boldsymbol{y}^*)$ related to the second-order terms, i.e. $L_{\boldsymbol{y}^*}(\boldsymbol{v}\boldsymbol{v}^T)$ yields the global optimal solution of (4) i.e. $\boldsymbol{v}^* = \sqrt{\lambda_1}\boldsymbol{\eta}_1$ where λ_1 is the non-zero eigenvalue and $\boldsymbol{\eta}_1$ is the corresponding eigenvector. Even if the rank-1 condition is not strictly satisfied, the above formula produces an approximate solution with λ_1 denoting the largest eigenvalue.

The whole method only needs minor modification to deal with rational objective functions. For $f(\boldsymbol{v}) = r(\boldsymbol{v})/s(\boldsymbol{v})$, modified problem (5) writes $\min_{\mu\in\mathscr{M}(\mathbb{K})_+} \int_{\mathbb{K}} r d\mu$ s.t. $\int_{\mathbb{K}} s d\mu = 1$. Accordingly, (7a) is modified to $L_{\boldsymbol{y}}(r)$ and (7e) is replaced by $L_{\boldsymbol{y}}(s) = 1$. In addition, the solution is extracted by $\boldsymbol{v}^* = \sqrt{\lambda_1}\boldsymbol{\eta}_1/\sqrt{\boldsymbol{y}^*(\boldsymbol{0})}$. This modification is based on method presented in [27].

V. Exploiting Sparsity in Moment Relaxations

IPF problem formulated as (1) is far from a generic polynomial problem but rather present some sparsity. If sparsity is properly exploited, it will lead to more efficient algorithm. In this section, we introduce the sparse moment relaxation developed in [29], [30] and applied to OPF in [21], [23]. Roughly speaking, this sparse moment relaxation rests on the observation that each equality or inequality constraint only involves a small subset of variables and the objective function can also be partitioned into polynomials involving only these small subsets of variables. Then under proper restriction on these subsets, the matrix equalities and inequalities in moment relaxation (7) can be decomposed into several smaller parts.

The sparsity in IPF problem (1) is precisely defined as follows. The sparsity of (1) is described in terms of an $n_b \times n_b$ symmetric symbolic matrix $\boldsymbol{R}$. Its element R_{ij} is 1 if and only if either (i) $i = j$, or (ii) $\boldsymbol{v}_i$ and $\boldsymbol{v}_j$ appear simultaneously in p_k or q_k for some $k \in \mathcal{N}$. All other elements of $\boldsymbol{R}$ are zeros. Note that condition (ii) above actually means either bus i and bus j are connected or they both connect to a third bus. IPF problem (1) is sparse if matrix $\boldsymbol{R}$ is sparse. To reduce the size of moment relaxation (7), the set of indexes of decision variables $\mathcal{N}$ needs to be partitioned into several possibly overlapping subsets according to the sparsity pattern of $\boldsymbol{R}$. The sparsity pattern graph of $\boldsymbol{R}$ is a undirected graph $G(\mathcal{N}, \mathcal{E})$ with $\mathcal{E} = \{(i,k) | i,k \in \mathcal{N}, i < k, R_{ik} = 1\}$.

Let $\mathcal{N}$ be the union $\cup_{i=1}^{p} \mathcal{N}_i$ of p possibly overlapping subsets $\mathcal{N}_i, i = 1, \ldots, p$. Define the sets of supports $\mathcal{A}^{\mathcal{N}_i} = \{\boldsymbol{\alpha} \in \mathbb{N}^{2n_b} | \alpha_{2k-1} = 0, \alpha_{2k} = 0, \forall k \notin \mathcal{N}_i\}$ and $\mathcal{A}_{2d}^{\mathcal{N}_i} = \{\boldsymbol{\alpha} \in \mathbb{N}_{2d}^{2n_b} | \alpha_{2k-1} = 0, \alpha_{2k} = 0, \forall k \notin \mathcal{N}_i\}$. Assume the partition $\mathcal{N} = \cup_{i=1}^{p} \mathcal{N}_i$ satisfies

$$\forall k \in \mathcal{N},\ \exists\ \mathcal{N}_i,\ \text{supp}(p_k) \subseteq \mathcal{A}^{\mathcal{N}_i} \text{ and } \text{supp}(q_k) \subseteq \mathcal{A}^{\mathcal{N}_i}. \quad (8)$$

Subsequently, $\mathcal{N}$ can be partioned into p disjoint sets $\mathcal{J}_i \subseteq \mathcal{N}_i, i = 1, \ldots, p$ such that $\forall 1 \le i \le p, \forall k \in \mathcal{J}_i, \text{supp}(p_k) \subseteq \mathcal{A}^{\mathcal{N}_i}$ and $\text{supp}(q_k) \subseteq \mathcal{A}^{\mathcal{N}_i}$, which can be done by assigning k to $\mathcal{J}_h$ such that $\mathcal{N}_h$ is the smallest set among all $\mathcal{N}_i$ satisfying $\text{supp}(p_k) \subseteq \mathcal{A}^{\mathcal{N}_i}$ and $\text{supp}(q_k) \subseteq \mathcal{A}^{\mathcal{N}_i}$. Observe that the set $\mathcal{C}_k = \{i \in \mathcal{N} |\ p_k \text{ involves } \boldsymbol{v}_i\}$ forms a clique of $G(\mathcal{N}, \mathcal{E})$ by definition of $\boldsymbol{R}$. Hence $\mathcal{C}_k$ is contained in one maximal clique of $G(\mathcal{N}, \mathcal{E})$. In light of this, assumption (8) can be satisfied if each $\mathcal{N}_i$ is a maximal clique of $G(\mathcal{N}, \mathcal{E})$. In addition, assume that for every $i = 1, \ldots, p-1$,

$$\exists\ r \in \{1, \ldots, i\},\ \mathcal{N}_{i+1} \cap (\mathcal{N}_1 \cup \cdots \cup \mathcal{N}_i) \subseteq \mathcal{N}_r. \quad (9)$$

Assumption (9) is known as the running intersection property in graph theory, which is satisfied when $\mathcal{N}_1, \ldots, \mathcal{N}_p$ are the maximal cliques of a chordal graph [31]. The following strategy is proposed in [29] to obtain a partition of $\mathcal{N}$ satisfying both (8) and (9). First, generate a chordal extension $G(\mathcal{N}, \mathcal{E}')$ of the graph $G(\mathcal{N}, \mathcal{E})$. Then find all maximal cliques $\mathcal{N}_i, i = 1, \ldots, p$ of $G(\mathcal{N}, \mathcal{E}')$. For implementation convenience, the above strategy can be realized through Cholesky factorization of $\boldsymbol{R} + \delta \boldsymbol{I}$ after a symmetric approximate minimum degree ordering, and the sparse pattern of the Cholesky factor defines the variable partition.

Under condition (8) and (9), the following sparse moment relaxation is well-defined with its optimum also converging to the global optimum of the original problem [27]:

$$\min_{\boldsymbol{y} \in \mathbb{R}^{\binom{2n_b+2d}{2d}}} L_{\boldsymbol{y}}(f) \qquad \text{subject to} \quad (10a)$$

$$M_{d_i}(\boldsymbol{y}, \mathcal{N}_i) \succcurlyeq \boldsymbol{0} \quad \forall 1 \le i \le p \quad (10b)$$

$$M_{d_i - d_{h_m}}(h_m \boldsymbol{y}, \mathcal{N}_i) = \boldsymbol{0} \quad \forall 1 \le i \le p, \forall m \in \mathcal{E}_i \quad (10c)$$

$$M_{d_i - d_{g_n}}(g_n \boldsymbol{y}, \mathcal{N}_i) \succcurlyeq \boldsymbol{0} \quad \forall 1 \le i \le p, \forall n \in \mathcal{I}_i \quad (10d)$$

$$y(\boldsymbol{0}) = 1 \quad (10e)$$

where $M_d(\boldsymbol{y}, \mathcal{N}_i)$ is the moment submatrix obtained from $M_d(\boldsymbol{y})$ by retaining those rows and columns indexed by $\boldsymbol{\alpha} \in \mathcal{A}_d^{\mathcal{N}_i}$; similarly, $M_d(h_m \boldsymbol{y}, \mathcal{N}_i)$ and $M_d(g_n \boldsymbol{y}, \mathcal{N}_i)$ are localizing submatrices obtained from $M_d(h_m \boldsymbol{y})$ and $M_d(g_n \boldsymbol{y})$ by retaining those rows and columns indexed by $\boldsymbol{\alpha} \in \mathcal{A}_d^{\mathcal{N}_i}$; $\mathcal{E}_i$ (resp. $\mathcal{I}_i$) denotes the index set of inequality (resp. equality) constraints (1b,1c,1f) (resp. (1d,1e)) with $k \in \mathcal{J}_i$. The sparse moment relaxation is exact if rank $M_{d_i}(\boldsymbol{y}, \mathcal{N}_i) = 1, \forall 1 \le i \le p$. The voltage $\boldsymbol{v}_k$ can then be extracted from the spectral decomposition of the diagonal block corresponding to second-order monomials in $M_{d_i}(\boldsymbol{y}, \mathcal{N}_i)$ where $k \in \mathcal{J}_i \subseteq \mathcal{N}_i$. The sizes of positive semidefinite constraints in (10) are considerably smaller than those of (7) due to the sparsity of $\boldsymbol{R}$. Hence it can be solved more efficiently and applied to cases larger than (7).

VI. Case Studies

To demonstrate the applicability and analyze the performance of moment-SOS approach to IPF problems, numerical studies are conducted on several IEEE standard systems. All the test data is extracted from MATPOWER 4.1 [32]. Moment-SOS approach is programmed in MATLAB with YALMIP [33] as the modeling tool and Mosek [34] as the solver. The program runs on a Win8 PC with a 3.0 GHz CPU with 8GB RAM. For brevity, PV-PQ bus type switching is not conducted in the followed case studies.

A. Exact Global Solutions on Small Cases

The sparse moment relaxation discussed above is directly applied to small-size IEEE 6-bus, 9-bus, and 14-bus systems with $\pm 10\%$ uncertainty on the loads to check whether moment-SOS approach can obtain the exact global interval power flow solutions. Two metrics are used to measure the global optimality of the solutions. The first metric is the smallest ratio between the largest and the second largest eigenvalues of all the moment matrices $M_{d_i}(\boldsymbol{y}, \mathcal{N}_i)$. The second metric is the largest violation of the extracted solution $\boldsymbol{v}^*$ to the constraints (1b)$\sim$(1f). The moment-SOS approach attains the global optimal solution if the first metric is large enough which certifies the satisfaction of the rank-1 condition and the second metric is small enough which certifies the feasibility of the extracted solutions.

Some numerical results are reported in Table I where column 3 and 4 show the extracted interval solutions, column 5 is the smallest value of the first metric related to the four problems in the same row, column 6 shows the largest value

of the second metric related to the four problems in the same row, and the last column shows the relaxation order needed to achieve these results. The notations V.M., V.A., A.P. and R.P. denote the bus voltage magnitude, the bus voltage angle, the line active power and the line reactive power, respectively. For all the problems shown in Table I, the values of the first metric are larger than 10e7 and the values of the second metric are smaller than 10e-6, which numerically certifies the global optimality of the extracted solutions. All the problems can be solved globally with the second-order moment relaxations. A small portion of problems can be solved with the first-order moment relaxations. Interestingly, all the max. V.M. problems are solved with first-order relaxation, and some max. A.P. and R.P. problems are also solved with first-order relaxation.

It is worth emphasizing the functionality of constraint (1f). In the implementation, the value of V_m^2 is set to be 0.5 p.u.. For example, with constraint (1f), the lower bound of the V.M. of bus 5 on IEEE-9 system is 0.9679 p.u. obtained by second-order moment relaxation. If constraint (1f) is dropped, the lower bound of V.M. of this bus is 0.0787 which can be obtained by first-order moment relaxation with the first metric 7.3e5 and the second metric 2.8e-6. Due to the existence of multiple solutions of power flow equations, one of the low voltage solutions is obtained if constraint (1f) is not added to problem (1). In addition, the constraint (1f) is not explicitly active (all the voltage magnitudes are strictly larger than 0.5 p.u.) which shows the complex nonlinear nature of power flow equations.

The exact interval power flow solutions of IEEE-9 and IEEE-14 systems are also shown in Fig. 1 and Fig. 2. Some inconsistency is observed between our results and the results reported in paper [12] on IEEE-9 system. Since this paper shares the same problem formulations with [12] (see eq. (6)∼(10) in [12]), the interval solution obtained by LP relaxation in paper [12] should not be tighter than the theoretically guaranteed exact interval solution obtained by moment-SOS approach in this paper. However, a brief comparison shows some results in [12] are even tighter than the results shown in Table I in this paper. The possible reason is that the initial estimation of the solution interval in [12] is so aggressive that it excludes the real global solutions.

B. High Accuracy Solution on Larger Cases

Even though sparsity is exploited, second-order moment relaxation for systems with more than forty buses is still numerically intractable using current SDP solvers. As shown from Table I, the first moment relaxation is only exact on very limited portion of cases. Therefore, generally speaking, only approximate solutions can be obtained for larger systems at the current stage. However, OBBT discussed in [12] and selective application of high-order constraints proposed in [23] can help to obtain very tight interval solutions.

The moment relaxation discussed in this paper can be used at the final stage of the algorithm framework discussed in [12], which means the LP relaxation based OBBT is firstly used to obtain the convex outer approximation of the feasible set (conceptually, SDP based OBBT can also be used, but it is too expensive). Then moment relaxation can be employed to solve the final problem and obtain the lower and upper bounds of related objectives. To this end, the following constraints

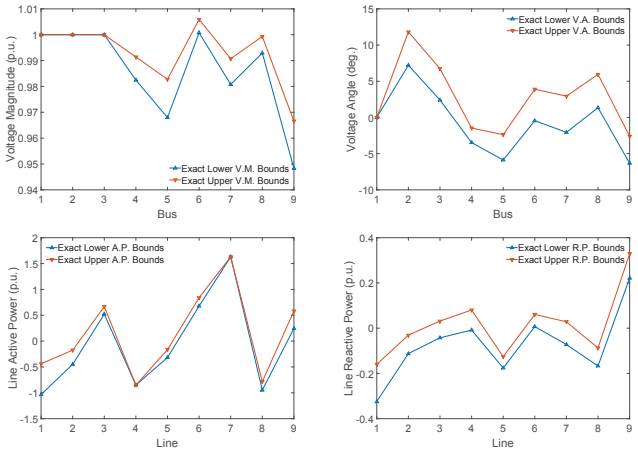

Fig. 1. Exact Interval Power Flow Bounds for IEEE-9 System

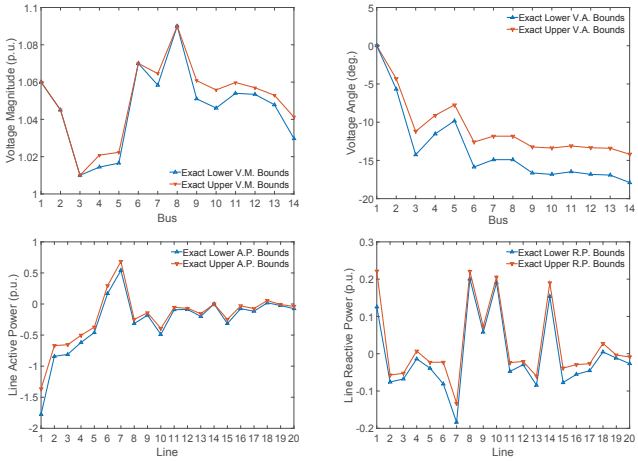

Fig. 2. Exact Interval Power Flow Bounds for IEEE-14 System

$$\underline{v}_i \le v_i \le \overline{v}_i \tag{11a}$$
$$v_i v_j - \underline{v}_i v_j - \underline{v}_j v_i + \underline{v}_i \underline{v}_j \ge 0, \quad (i,j) \in \mathcal{L} \tag{11b}$$
$$v_i v_j - \overline{v}_i v_j - \overline{v}_j v_i + \overline{v}_i \overline{v}_j \ge 0, \quad (i,j) \in \mathcal{L} \tag{11c}$$
$$v_i v_j - \underline{v}_i v_j - \overline{v}_j v_i + \underline{v}_i \overline{v}_j \le 0, \quad (i,j) \in \mathcal{L} \tag{11d}$$
$$v_i v_j - \overline{v}_i v_j - \underline{v}_j v_i + \overline{v}_i \underline{v}_j \le 0, \quad (i,j) \in \mathcal{L} \tag{11e}$$

need to be added to the polynomial problem (1) before construct the moment relaxation.

The solutions obtained from the first-order moment relaxation satisfy or slightly violate most of the constraints (1b)∼(1f). Only very limited number of constraints are considerably violated. Therefore selectively apply high-order relaxation to these buses where large violation happens may significantly tighten the relaxation. To this end, each bus is associated with a relaxation order and the relaxation order of the maximal clique $\mathcal{N}_i$ is equal to the highest order of buses in $\mathcal{J}_i$. In this way, (10b) is constructed according to the order of the maximal clique and (10c)∼(10d) are constructed according

TABLE I
EXACT INTERVAL POWER FLOW SOLUTIONS FOR 6, 9 AND 14-BUS SYSTEMS UNDER 10% LOAD UNCERTAINTY

System	Bus/Line	V.M./A.P.	V.A./R.P.	min eig. ratio	max con. violation	relaxation order			
6-bus	4	[0.9819, 0.9967]	[-5.2053,-3.1978]	7.8e+8	7.4e-9	2nd	1st	2nd	2nd
	5	[0.9762, 0.9944]	[-6.5193,-4.0450]	1.6e+9	7.1e-9	2nd	1st	2nd	2nd
	6	[0.9973, 1.0114]	[-7.4406,-4.4832]	8.2e+8	9.4e-9	2nd	1st	2nd	2nd
	1-2	[-0.3712,-0.2055]	[0.0969, 0.1668]	4.2e+9	3.7e-9	2nd	1st	2nd	2nd
	2-6	[-0.3048,-0.2206]	[-0.1817,-0.1221]	4.6e+8	3.1e-8	2nd	2nd	2nd	1st
	4-5	[-0.0679,-0.0140]	[-0.0121, 0.0323]	2.5e+9	2.6e-9	2nd	2nd	2nd	2nd
9-bus	5	[0.9679, 0.9828]	[-5.8822,-2.1736]	1.5e+8	6.4e-8	2nd	1st	2nd	2nd
	7	[0.9801, 0.9908]	[-2.0765, 3.2822]	2.4e+8	3.4e-8	2nd	1st	2nd	2nd
	9	[0.9483, 0.9666]	[-6.3340,-2.3979]	1.5e+8	6.3e-8	2nd	1st	2nd	2nd
	1-4	[-1.0352,-0.4059]	[-0.3266,-0.1579]	8.5e+7	2.7e-7	2nd	1st	2nd	1st
	5-6	[0.5215, 0.6671]	[-0.0438, 0.0316]	1.7e+8	4.0e-8	2nd	2nd	2nd	2nd
	8-9	[-0.9477,-0.7825]	[-0.1670,-0.0877]	4.6e+8	3.5e-8	2nd	2nd	2nd	2nd
14-bus	4	[1.0144, 1.0208]	[-11.5329,-9.1053]	1.5e+8	1.7e-8	2nd	1st	2nd	2nd
	7	[1.0584, 1.0646]	[-14.9016,-11.8320]	1.1e+8	1.7e-8	2nd	1st	2nd	2nd
	13	[1.0478, 1.0529]	[-16.9197,-13.4119]	2.5e+7	4.9e-8	2nd	1st	2nd	2nd
	2-5	[-0.4582,-0.3725]	[-0.0387,-0.0230]	5.8e+7	4.5e-7	2nd	2nd	2nd	1st
	6-13	[-0.1989,-0.1561]	[-0.0842,-0.0603]	7.8e+7	3.6e-8	2nd	2nd	2nd	1st
	9-10	[-0.0745,-0.0300]	[-0.0553,-0.0291]	2.9e+8	9.5e-8	2nd	2nd	2nd	2nd

to the order of the buses. In our implementation, for all bus $k \in \mathcal{J}_i \subseteq \mathcal{N}_i$ with $|\mathcal{N}_i| \leq 8$, second-order relaxations are applied to two buses where the solution to first-order relaxation yields largest violation.

We have conducted comparative case studies among LP relaxation, first-order moment relaxation (denoted as ord-1 MR) and first-order moment relaxation with 2 second-order buses (denoted as ord-1.2 MR) on IEEE-57 and IEEE-118 systems with $\pm 10\%$ uncertainty on the loads. All the problems are solved by each method after exactly the same LP based OBBT procedure. Some numerical results are reported in Table II and Table III. It clearly shows that ord-1 MR obtains tighter interval solutions than LP, and ord-1.2 MR obtains tighter interval solutions than ord-1 MR. The OBBT procedure really help to tighten the initial estimation of the solution interval so that the LP relaxation already obtains quite tight interval solutions on many cases. However, large improvement of ord-1 MR compared with LP is still observed on several cases, especially for the upper bounds of the line reactive power. For example, the upper bound for the reactive power of line 6-7 on IEEE-57 system obtained by LP is 0.4179 p.u., while that obtained by ord-1 MR is 0.0392. The upper bound of reactive power of line 4-5 on IEEE-118 system acquired by LP is 2.2667 compared to 0.2972 acquired by ord-1 MR. The improvement from ord-1 MR to ord-1.2 MR is not so significant compared with that from LP to ord-1 MR. Of course, increasing the number of second-order buses will further tighten the interval solutions but the marginal benefits will quickly diminish as shown in the comparison among LP, ord-1 MR and ord-1.2 MR. The interval power solutions obtained by ord-1.2 MR on IEEE-57 system is also shown in Fig. 3.

TABLE II
COMPARISON OF BOUNDS SOLUTION ON 57-BUS SYSTEM

Problem	LP	ord-1 MR	ord-1.2 MR
4 V.M.	[0.9672,0.9941]	[0.9676,0.9816]	[0.9685,0.9816]
4 V.A.	[-11.1053,-3.3970]	[-11.0289,-4.4419]	[-11.0258,-4.4430]
7 V.M.	[0.9578,1.0119]	[0.9582,0.9863]	[0.9592,0.9863]
7 V.A.	[-13.3077,-1.4924]	[-13.1830,-3.0075]	[-13.1803,-3.0798]
3-4 A.P.	[-1.0530,-0.1512]	[-0.9706,-0.3440]	[-0.9503,-0.3461]
3-4 R.P.	[-0.5194,0.5746]	[-0.4804,0.1475]	[-0.4797,0.1472]
6-7 A.P.	[-0.1428,0.5148]	[0.0013,0.3664]	[0.0026,0.3336]
6-7 R.P.	[-0.4303,0.4179]	[-0.4036,0.0392]	[-0.3898,0.0389]

TABLE III
COMPARISON OF BOUNDS SOLUTION ON 118-BUS SYSTEM

Problem	LP	ord-1 MR	ord-1.2 MR
2 V.M.	[0.9612,0.9810]	[0.9612,0.9720]	[0.9675,0.9720]
2 V.A.	[-22.4996,-14.3718]	[-22.3451,-14.4066]	[-22.3443,-14.6189]
5 V.M.	[0.9927,1.0106]	[0.9930,1.0022]	[0.9938,1.0022]
5 V.A.	[-17.6181,-10.2282]	[-17.4044,-10.2582]	[-17.4041,-10.4862]
4-5 A.P.	[0.7346,1.3359]	[0.8414,1.2374]	[0.8883,1.1936]
4-5 R.P.	[-1.9190,2.2667]	[-1.8780,0.2912]	[-1.7711,0.2866]
5-6 A.P.	[-1.2543,-0.5347]	[-1.1742,-0.7266]	[-1.0978,-0.7631]
5-6 R.P.	[-0.2928,0.1884]	[-0.2020,0.1121]	[-0.2008,0.0995]

C. IEEE 300-bus System with Wind Power

The proposed method is also applied to IEEE 300-bus system with wind power uncertainties. Partial diagram of the system configuration is shown in Fig. 4. Three wind farms are installed at bus 225, 231 and 237 of the standard 300-bus system. Each wind farm has a power capacity of 80MW. The actual output power of each wind farm possesses $\pm 20\%$ uncertainty in terms of its capacity. The reactive power compensation devices and related control system in each wind farm always maintain a power factor of 1 at the connection point. Ord-1 MR is employed to obtain the interval solutions on several buses and lines which are heavily affected by the uncertain output of wind farms. LP relaxation method is also introduced for comparison. Results are shown in Fig. 5 which demonstrates the proposed method can obtain much tighter interval solutions than LP relaxation method.

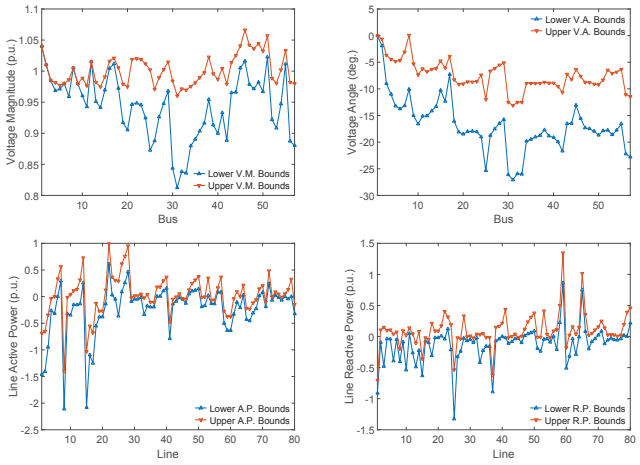

Fig. 3. Interval Solutions by ord-1.2 MR on IEEE-57 System

TABLE IV
SOLVER TIME COMPARISON (SEC.)

System	LP	ord-1 MR	ord-1.2 MR	ord-2MR
9-bus	0.17	0.2	2.3	3.64
14-bus	0.17	0.34	41.58	67.14
57-bus	0.27	2.47	30.98	/
108-bus	0.36	6.11	69.88	/

TABLE V
SOLVER TIME FOR ORD-1 MR (SEC.)

Exploit Sparsity	Systems					
	6	9	14	57	118	300
Yes	0.17	0.20	0.34	2.47	6.11	9.19
No	0.17	0.25	0.36	187	3346	intractable

D. Performance Analysis

Interval widths obtained by different relaxation methods are compared in Fig. 6, Fig. 7 and Fig. 8. Since the ord-2 MR obtains the exact interval solutions on IEEE-9 and IEEE-14 bus systems, the solid black line on Fig. 6 and Fig. 7 represent the exact interval widths. The ord-2 MR is numerically intractable for IEEE-57 system, so only LP, ord-1 MR and ord-1.2 are drawn in Fig. 8. It is observed that the bound tightening effects of MRs compared with LP are generally very significant on line reactive power problems but much less significant on bus voltage angle problems. As shown in Fig. 6 and Fig. 7, the four lines of the voltage angles almost coincide with each other whereas the four lines of the line reactive power exhibit considerable differences. As system scale increases, the gaps between LP and MRs intensifies. As shown in Fig. 8, the LP relaxation yields very conservative interval solutions for some line active and reactive power problems. The difference between ord-1 MR and ord-1.2 MR is almost overwhelmed by the difference between LP and ord-1 MR, so the lines for ord-1 MR and the lines for ord-1.2 MR nearly coincide with each other in Fig. 8. The possible explanation for this phenomenon is that the severe non-linearity of line power functions may prevent LP relaxation makes a good approximation to optimization problem to be solved.

The bound tightening benefits of MRs compared with LP, of course, are not without costs. Typical solver time for a single problem needed for different methods is listed in Table IV. Since the sizes of the linear matrix inequality constraints increase dramatically as the system scale and relaxation order increase, the solver time needed for MRs increases significantly as the system scale and number of second-order buses increase.

Note that the SDP relaxation (equivalent to ord-1 MR [23]) for OPF problems is demonstrated applicable to systems with more than 3000 buses [18]. Therefore, the ord-1 MR should be considered as a practical remedy for LP relaxation if high accuracy interval solutions are needed. Moreover, for small-size systems, the ord-2 MR can give theoretically guaranteed exact interval solutions in stark contrast to the outer approximate given by IA, AA and LP methods and the inner approximation given by Monte Carlo simulation. When developing new methods, the results obtained by ord-2 MR are better standard results used for comparison than results given by Monte Carlo method often used in the literature.

Finally, We evaluate the effects of the sparsity-exploiting technique presented in Section V. Fig. 9 illustrates the partition of buses on IEEE 9-bus system. All buses are partitioned into 5 overlapping cliques and the largest clique contains 5 buses. Under this partition, the size of the largest SDP constraint for ord-2 MR (ord-1 MR) will decrease from 190×190 (19×19) to 66×66 (11×11). When this techniques is applied to IEEE 300-bus system, the size of the largest SDP constraint for ord-1 MR will decrease from 601×601 to 39×39. Such significant reduction of constraint sizes will result in shorter solver time and higher tractability. The comparison of solver time needed before and after applying the sparisity exploiting technique is shown in Table V and Table VI. Since IEEE 6-bus system can only be partitioned into one clique, the sparsity-exploiting technique has no influence on its solution process and time. For other cases, it is shown that the sparsity-exploiting technique has brought orders-of-magnitude solver time saving for ord-1 MR on larger systems and for ord-2 MR even on small systems.

VII. CONCLUSIONS

In this paper, moment-SOS approach is applied to interval power flow analysis which is formulated as polynomial optimization problems. Correlative sparsity of the problem formulation is exploited to improve numerical tractability and

TABLE VI
SOLVER TIME FOR ORD-2 MR (SEC.)

Exploit Sparsity	Systems		
	6	9	14
Yes	5.26	3.64	67.14
No	5.26	81.03	7385

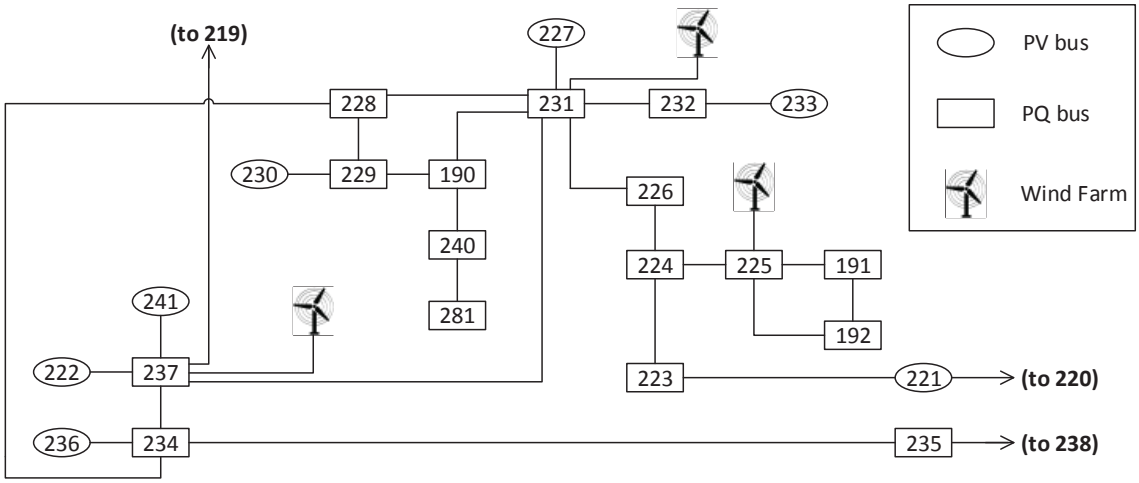

Fig. 4. Partial Diagram of IEEE 300-bus System with Wind Farms

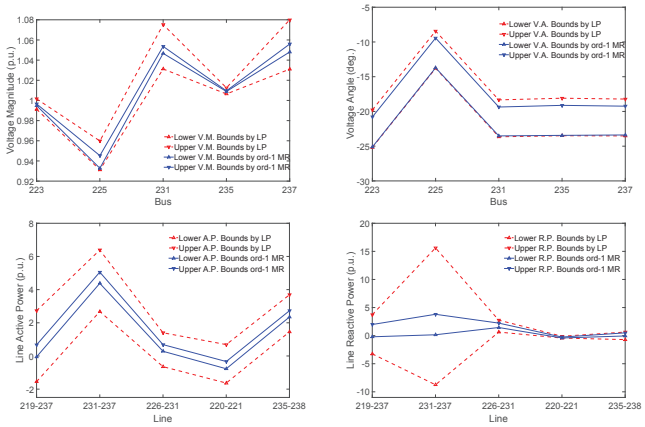

Fig. 5. Comparison of ord-1 MR and LP on IEEE 300-bus System

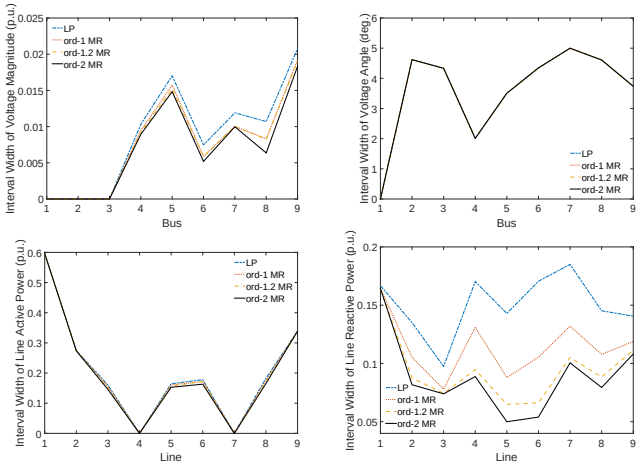

Fig. 6. Interval Width for IEEE-9 System Using Different Methods

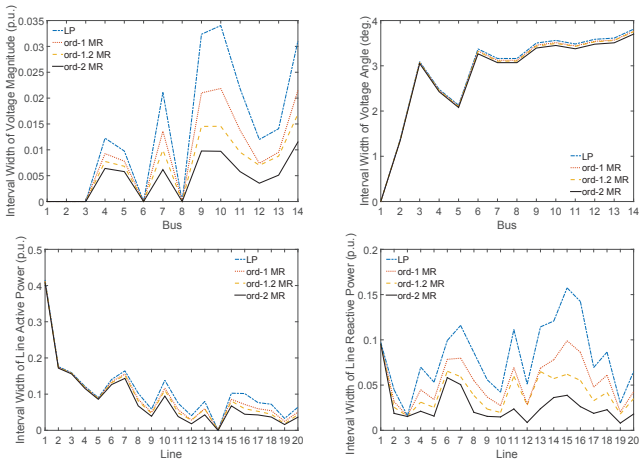

Fig. 7. Interval Width for IEEE-14 System Using Different Methods

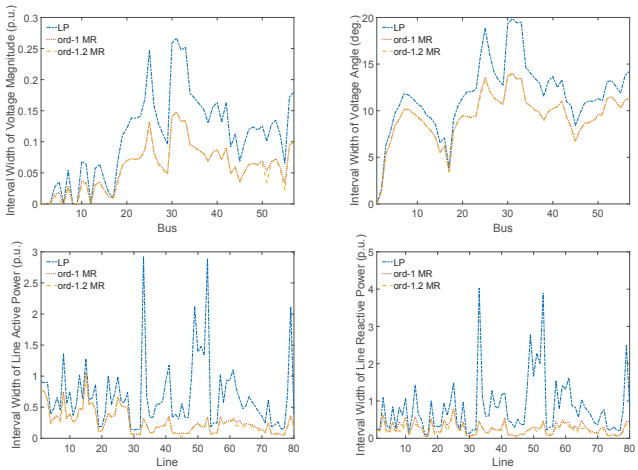

Fig. 8. Interval Width for IEEE-57 System Using Different Methods

efficiency. Numerical studies on IEEE 6-bus, 9-bus and 14-bus systems demonstrate this approach is capable of obtaining exact interval solutions on small-scale systems. Moreover, this approach can significantly improve the interval solutions on larger systems based on numerical studies on IEEE 57-bus, 118-bus and 300-bus systems.

Note that the improvement of solution accuracy is at the cost

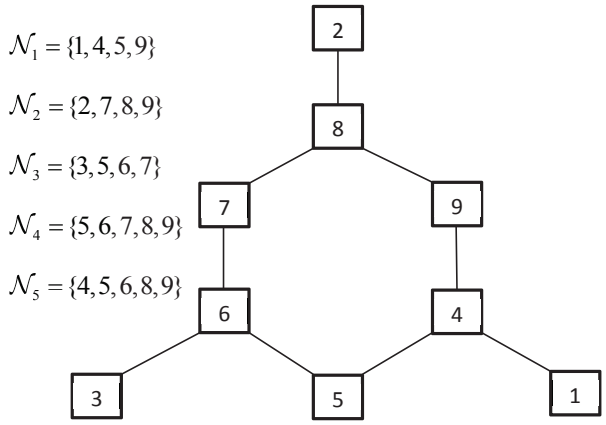

Fig. 9. Partition of Buses on IEEE 9-bus System

of longer solver time. Therefore, future research will focus on two directions. First, seek for other approaches to construct convex relaxations for IPF problems where the complexity can be systematically controlled, so that it is flexible to choose suitable convex relaxation considering the tradeoff between accuracy and solver time. Second, speed up the computation by exploiting the separability in the algorithm which allows for parallel computing.

REFERENCES

[1] H. Yu, C. Chung, K. Wong, H. Lee, and J. Zhang, "Probabilistic load flow evaluation with hybrid latin hypercube sampling and cholesky decomposition," *IEEE Trans. Power Syst.*, vol. 24, pp. 661–667, May 2009.

[2] M. Hajian, W. Rosehart, and H. Zareipour, "Probabilistic power flow by monte carlo simulation with latin supercube sampling," *IEEE Trans. Power Syst.*, vol. 28, pp. 1550–1559, May 2013.

[3] R. Allan, A. Leite da Silva, and R. Burchett, "Evaluation methods and accuracy in probabilistic load flow solutions," *IEEE Trans. Power App. Syst.*, vol. PAS-100, pp. 2539–2546, May 1981.

[4] P. Zhang and S. Lee, "Probabilistic load flow computation using the method of combined cumulants and gram-charlier expansion," *IEEE Trans. Power Syst.*, vol. 19, pp. 676–682, Feb 2004.

[5] Z. Hu and X. Wang, "A probabilistic load flow method considering branch outages," *IEEE Trans. Power Syst.*, vol. 21, pp. 507–514, May 2006.

[6] C.-L. Su, "Probabilistic load-flow computation using point estimate method," *IEEE Trans. Power Syst.*, vol. 20, pp. 1843–1851, Nov 2005.

[7] J. Morales and J. Perez-Ruiz, "Point estimate schemes to solve the probabilistic power flow," *IEEE Trans. Power Syst.*, vol. 22, pp. 1594–1601, Nov 2007.

[8] Z. Wang and F. Alvarado, "Interval arithmetic in power flow analysis," *IEEE Trans. Power Syst.*, vol. 7, pp. 1341–1349, Aug 1992.

[9] A. Dimitrovski and K. Tomsovic, "Boundary load flow solutions," *IEEE Trans. Power Syst.*, vol. 19, pp. 348–355, Feb 2004.

[10] A. Vaccaro, C. Canizares, and D. Villacci, "An affine arithmetic-based methodology for reliable power flow analysis in the presence of data uncertainty," *IEEE Trans. Power Syst.*, vol. 25, pp. 624–632, May 2010.

[11] A. Vaccaro, C. Canizares, and K. Bhattacharya, "A range arithmetic-based optimization model for power flow analysis under interval uncertainty," *IEEE Trans. Power Syst.*, vol. 28, pp. 1179–1186, May 2013.

[12] T. Ding, R. Bo, F. Li, Q. Guo, H. Sun, W. Gu, and G. Zhou, "Interval power flow analysis using linear relaxation and optimality-based bounds tightening (obbt) methods," *IEEE Trans. Power Syst.*, vol. 30, pp. 177–188, Jan 2015.

[13] J. A. Taylor, *Convex Optimization of Power Systems*. Cambridge University Press, 2015.

[14] J. Lavaei and S. Low, "Zero duality gap in optimal power flow problem," *IEEE Trans. Power Syst.*, vol. 27, pp. 92–107, Feb 2012.

[15] L. Gan, N. Li, U. Topcu, and S. Low, "Exact convex relaxation of optimal power flow in radial networks," *IEEE Trans. Autom. Control*, vol. 60, pp. 72–87, Jan 2015.

[16] R. Madani, S. Sojoudi, and J. Lavaei, "Convex relaxation for optimal power flow problem: Mesh networks," *IEEE Trans. Power Syst.*, vol. 30, pp. 199–211, Jan 2015.

[17] R. Jabr, "Exploiting sparsity in sdp relaxations of the opf problem," *IEEE Trans. Power Syst.*, vol. 27, pp. 1138–1139, May 2012.

[18] D. Molzahn, J. Holzer, B. Lesieutre, and C. DeMarco, "Implementation of a large-scale optimal power flow solver based on semidefinite programming," *IEEE Trans. Power Syst.*, vol. 28, pp. 3987–3998, Nov 2013.

[19] J. B. Lasserre, "Global optimization with polynomials and the problem of moments," *SIAM Journal on Optimization*, vol. 11, no. 3, pp. 796–817, 2001.

[20] J. Nie, "Optimality conditions and finite convergence of lasserres hierarchy," *Mathematical programming*, vol. 146, no. 1-2, pp. 97–121, 2014.

[21] B. Ghaddar, J. Marecek, and M. Mevissen, "Optimal power flow as a polynomial optimization problem," *IEEE Trans. Power Syst.*, vol. PP, pp. 1–8, Jan 2015.

[22] C. Josz, J. Maeght, P. Panciatici, and J. Gilbert, "Application of the moment-SOS approach to global optimization of the opf problem," *IEEE Trans. Power Syst.*, vol. 30, pp. 463–470, Jan 2015.

[23] D. Molzahn and I. Hiskens, "Sparsity-exploiting moment-based relaxations of the optimal power flow problem," *IEEE Trans. Power Syst.*, vol. 30, pp. 3168–3180, Nov 2015.

[24] Y. Tamura, H. Mori, and S. Iwamoto, "Relationship between voltage instability and multiple load flow solutions in electric power systems," *IEEE Trans. Power App. Syst.*, no. 5, pp. 1115–1125, 1983.

[25] X. Wang and Y. Song and M. Irving, *Modern power systems analysis*, Springer Science & Business Media, 2010.

[26] G. Blekherman, P. A. Parrilo, and R. R. Thomas, *Semidefinite optimization and convex algebraic geometry*, vol. 13. Siam, 2013.

[27] J.-B. Lasserre, *Moments, positive polynomials and their applications*, vol. 1. World Scientific, 2009.

[28] S. Kim, M. Kojima, and H. Waki, "Generalized lagrangian duals and sums of squares relaxations of sparse polynomial optimization problems," *SIAM Journal on Optimization*, vol. 15, no. 3, pp. 697–719, 2005.

[29] H. Waki, S. Kim, M. Kojima, and M. Muramatsu, "Sums of squares and semidefinite program relaxations for polynomial optimization problems with structured sparsity," *SIAM Journal on Optimization*, vol. 17, no. 1, pp. 218–242, 2006.

[30] J. B. Lasserre, "Convergent sdp-relaxations in polynomial optimization with sparsity," *SIAM Journal on Optimization*, vol. 17, no. 3, pp. 822–843, 2006.

[31] J. R. Blair and B. Peyton, "An introduction to chordal graphs and clique trees," in *Graph theory and sparse matrix computation*, pp. 1–29, Springer, 1993.

[32] R. Zimmerman, C. Murillo-Sánchez, and R. Thomas, "Matpower: Steady-state operations, planning, and analysis tools for power systems research and education," *IEEE Trans. Power Syst.*, vol. 26, pp. 12–19, Feb 2011.

[33] J. Löfberg, "Yalmip : A toolbox for modeling and optimization in MATLAB," in *Proceedings of the CACSD Conference*, (Taipei, Taiwan), 2004.

[34] M. ApS, *The MOSEK optimization toolbox for MATLAB manual. Version 7.1 (Revision 28).*, 2015.

Chao Duan (S'14) was born in Chongqing, China, in 1989. He received the B.S. degree in electrical engineering from Xi'an Jiaotong University, Xi'an, China, in 2012. He is currently pursuing the Ph.D. degree at Xi'an Jiaotong University, Xi'an, China, and the University of Liverpool, Liverpool, U.K.

His research interests are in power system optimization and control.

Lin Jiang (M'00) received the B.Sc. and M.Sc. degrees from Huazhong University of Science and Technology (HUST), China, in 1992 and 1996; and the Ph.D. degree from the University of Liverpool, UK, in 2001, all in Electrical Engineering.

He worked as a Postdoctoral Research Assistant in the University of Liverpool from 2001 to 2003, and Postdoctoral Research Associate in the Department of Automatic Control and Systems Engineering, the University of Sheffield from 2003 to 2005. He was a Senior Lecturer at the University of Glamorgam from 2005 to 2007 and moved to the University of Liverpool in 2007. Currently, he is a Senior Lecturer in The University of Liverpool. His current research interests include control and analysis of power system, smart grid, and renewable energy.

Wanliang Fang was born in Henan, China, in 1958. He received the B.S. and M.S. degrees from Xi'an Jiaotong University, Xi'an, China in 1982 and 1988, respectively, and the Ph.D. degree from Hong Kong Polytechnic University, HongKong, in 1999, all in electrical engineering.

He is currently a Professor of electrical engineering at Xi'an Jiaotong University. His research interests include power system stability analysis and control, FACTS and HVDC.

Jun Liu (S'09-M'10) received the B.S. and Ph.D. degrees from Xi'an Jiaotong University, Xi'an, China, in 2004 and 2012, respectively, all in electrical engineering.

He is currently an Associate Professor with the Department of Electrical Engineering, Xi'an Jiaotong University, and he was a Visiting Scholar with Texas A&M University, College Station, TX, USA, from September 2008 to August 2010. His research interests include renewable energy integration, power system operation and control, power system stability, HVDC, and FACTS.